Solar Heating for Pit Thermal Energy Storage – Comparison of Solar Thermal and Photovoltaic Systems in TRNSYS 18

Klaudia Słomczyńska[1,2*], Paweł Mirek[2], Marcin Panowski[2]

[1] Energoprojekt-Katowice SA, ul. Jesionowa 15, 40-159 Katowice, Poland

[2] Faculty of Infrastructure and Environment, Czestochowa University of Technology, ul. J.H. Dąbrowskiego 69, 42-201 Częstochowa, Poland

* Corresponding author's e-mail: klaudia.zolinska@pcz.pl

ABSTRACT

Solar collectors and photovoltaic panels are devices widely used for heating water for both heating and domestic purposes. Due to the variable nature of solar radiation, it is advisable to include in solar energy-based systems thermal storages that accumulate energy at times of overproduction and discharge it at times of demand. In this paper, we present the results of simulation research to compare the possibility of two different charging systems for a 24000 m³ seasonal pit thermal energy storage. The first uses electricity generated by photovoltaic panels and converted to heat in an electrode boiler to charge the heat store. The second is utilising a solar collector for this purpose. Based on the simulation calculations carried out in TRNSYS 18, it can be concluded that, from an investment perspective, a system based on solar collectors is more cost-effective. In addition, the installation takes up less space compared to a photovoltaic panel farm.

Keywords: solar energy, district heating, heat storage system, pit thermal energy storage, TRNSYS.

INTRODUCTION

Fifty percent of global final energy consumption is for heating purposes [1]. However, due to progressive climate change, the exhaustion of fossil fuel resources and the increasing costs of conventional energy [2], the heating sector is facing an energy transformation. This transformation should use renewable energy sources, the most promising being solar thermal energy [3, 4].

Solar radiant energy can be used in district heating through photovoltaic panels (PV) and solar thermal (ST). Photovoltaic panels convert solar radiation into electrical energy [5], which can then be used, among other things, for conversion into heat according to the P2H (power-to-heat) method, e.g. electric boilers or heat pumps [6, 7]. The combination of PV with P2H technology devices has excellent economic and environmental potential [8, 9]. Much more common in district heating systems are solar collectors, which directly convert the sun's radiant energy into thermal energy [10–12].

The use of solar thermal systems is inextricably linked to the problem of intermittent energy production [13]. A solution to this problem is seasonal thermal storage [14, 15]. The use of thermal storage in district heating systems based on renewable energy sources removes the mismatch between heat production and heat demand. As a result, it alleviates the long periods of no or too low solar energy (e.g. night) and the short fluctuations in the availability of solar energy, which affect the stability of power and heat networks. It also makes it possible to combine several heating technologies into one system, e.g. solar collectors with CHP and P2H technology [16].

There are many different types of seasonal thermal storage, including sensible heat storage, latent heat storage and chemical storage. Sensible heat can be stored in hot water thermal energy storage (TTES), aquifer thermal energy storage

(ATES), water pit thermal energy storage (PTES) and borehole thermal energy storage (BTES) [13]. PTES is used in this study because it shows reasonable construction costs while being able to be built in almost any location [17].

Designing, predicting and analysing the performance of renewable energy systems that are strongly dependent on weather conditions is possible through computer simulations. Commonly used for the analysis of district heating installations is the TRNSYS simulation software, which makes it possible to carry out the transient simulation of systems. The Simulation Studio, part of the TRNSYS package, allows building entire energy systems by connecting individual component models (so-called components). Each component requires specific parameters and input data. The parameters are invariable throughout the simulation and define the general characteristics of the device, i.e. area or power rating. The input data are time-varying and can be read from an external file or transferred from another component. At each time step of the simulation, the component takes the input data and calculates the outputs from them. The simulation results can be followed in real-time in the form of graphs or downloaded in a text file after the calculation is completed. TRNSYS software is widely used in modelling solar and wind systems, cogeneration, hydrogen fuel cells, ground heat transfer or heat pump systems [17]. For example, Rehman at al. [13] used this software to compare five centralised and decentralised solar thermal systems for heating 100 houses on a housing estate in Finland. Renaldi et al. [19] used calculations in TRNSYS for techno-economic analysis of a solar thermal system with seasonal heat storage in the UK. TRNSYS can also be used to simulate the operation of systems with different types of heat stores, such as BTES [20–22], TTES [23, 24], ATES [25] and PTES [26].

This study aimed to compare the possibilities of charging the PTES storage tank with a capacity of 24 000 m^3 using two systems based on solar energy. System No. I is based on a photovoltaic panel farm, and system No. II is on a solar collector. The comparison is carried out in three different locations in Poland. The TRNSYS simulation software is used to estimate the parameters of both installations

METHODOLOGY

Two technologies are used to charge the seasonal heat storage: photovoltaic panels (PV) and solar thermal (ST). In order to compare them, two models are created: utilizing PV panels (configuration I) and ST (configuration II). Then, using simulation methods, the two installations' rated power is selected to charge the storage for three months (June, July and August). It is assumed that PTES is fully charged if the average water temperature is above 80°C. The calculations are carried out for three different locations in Poland: the central, northern and southern regions. These sites are chosen to test the ability of solar systems in different parts of the country to charge PTES heat storage. An additional criterion is the availability of weather data for these locations. Then two systems in each area are compared in energy and economic terms.

System description

The system's main component is pit thermal energy storage (PTES). PTES is a tank embedded in the ground and usually filled with water. The sides of the tank are covered with banks, which increase the total volume of the storage. Banks on the sides of the tank increase the total volume of the storage. At the top of the tank is an insulating lid. It floats on the surface or is supported by the lateral banks. Water in PTES is not kept under pressure, and it is designed to be stored at a temperature of 90–95°C [27, 28]. A schematic diagram of the PTES is shown in Figure 1.
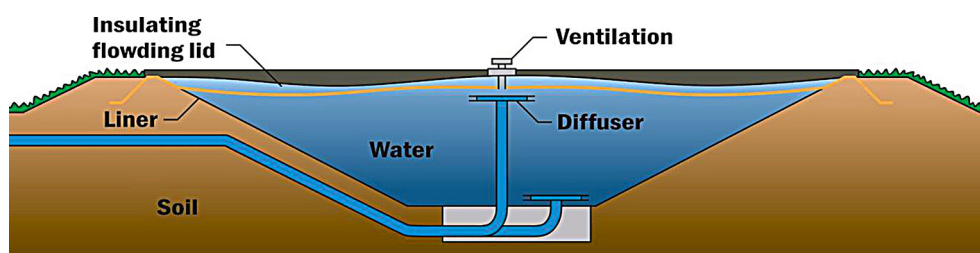

Figure 1. A schematic diagram of the pit thermal storage (PTES) [29]
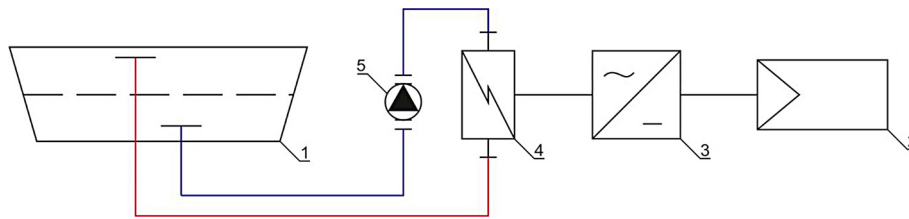
Figure 2. Technological diagram of system I utilizing PV as the energy source (1 – pit thermal energy storage, 2 – photovoltaic panel farm, 3 – inverter, 4 – electrode boiler, 5 – circulation pump)
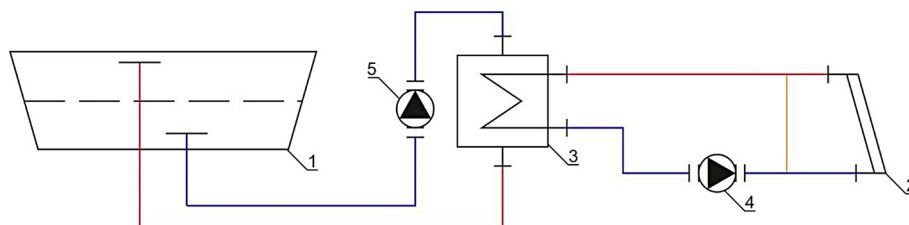

Figure 3. Technological diagram of system II utilizing solar thermal as the energy source, 1 – pit thermal energy storage, 2 – solar thermal farm, 3 – heat exchanger, 4 – water-glycol circulation pump, 5 – water circulation pump

The charging and discharging of the tank can be done simultaneously by pumping water into/out of the tank. During charging, water at a lower temperature is taken from the lower part of the tank. After being heated, it flows to the top of the tank. On the other hand, when unloading, warm water is taken from the upper part of the storage tank and then cooled and pumped into the lowest layers. This leads to stratification in the tank, i.e. the division of water into areas of different temperatures. As a result, a thermocline is formed between the warm water at the top of the tank and the cold water at the bottom. This is the transition layer which prevents water occurring in the layers above and below from mixing. When working with PTES, the aim is to prevent the hot and cold layers from mixing to reduce the heat loss throughout the tank [28, 30].

Two technological configurations are proposed to charge the PTES tank (1). Configuration No. I is shown in Figure 2 and consists of a PV farm (2), an electrode boiler (EB) (4) and a circulating pump (5). Configuration No. II is presented in Figure 3 and consists of a ST farm (2), a heat exchanger (HE) (3) and a circulating pumps for water (5) and water-glycol mixture (4).

Configuration No. I is based on the P2H concept. Water from the bottom of the heat storage is transferred to the electrode boiler, which functions as a flow heater and warms the water to a temperature of 90°C. After heating, the water is pumped to the top layer of the PTES. The PV farm generates electricity used by the electrode boiler. The most significant parameters of PV are shown in Table 1.

Configuration No. II is based on a system of solar collectors in which a water-glycol mixture circulates. When this mixture reaches a temperature above 90°C, it is transferred to a heat exchanger. Then, the waterflow from the lowest PTES layer is directed to the heat exchanger, where it is heated by the ST circuit working medium. If the temperature of the water-glycol mixture is too low, it bypasses the HE and returns to the thermal solar where it is heated. The most significant parameters of the solar thermals are presented in Table 2.

The rated power of the solar collectors (10.92 kW) is calculated based on the following equation [34]

$$P_{ST} = \eta_0 \cdot A_{active} \cdot E_g \qquad (1)$$

where: η_0 – optical efficiency [-],
A_{active} – active surface (aperture area) [m^2],
E_g – largest total solar irradiance, 1000 W/m^2.

Table 1. The most significant parameters of photovoltaic panels used in variant I [31]

Type	Monocrystalline
Rated power	500 Wp
Module efficiency	21.3%
Surface	2.35 m^2
Slope of surface	30
Azimuth of surface	0

Table 2. The most significant parameters of solar collectors used in variant II [32, 33]

Type	Large surface flat collector
Optical efficiency	0.77
Effective heat capacity	6483 J/m^{2}K
Active surface (aperture area)	14.18 m^2
Gross surface	15.50 m^2
Coefficient a1	2.23 W/m^{2}K
Coefficient a2	0.008 W/m^{2}K^2
Incidence-angle modifier IAM	0.91
Slope of surface	30
Azimuth of surface	0

Model

Configuration No. I – in this configuration, TRNSYS modules are used to simulate the work of the photovoltaic panels (Type190c), inverter (Type48a), electrode boiler (Type138), PTES tank (Type342_fixDP), pump (Type110), and pipelines (Type31). The simulation model is shown in Figure 4.

Configuration No. II – *fo*r configuration No. II the following TRNSYS models are used: solar collectors (Type832v501), splitter (Type11f), pumps (Type110), mixer (Type11h), heat exchanger (Type5b), PTES tank (Type342_fixDP). The schematic diagram of the PTES heat storage heating system model using solar collectors is shown in Figure 5.

Weather data

Meteorological data are necessary to perform simulation calculations for renewable energy systems. They are input data to the model using the Type99 component. During the simulation calculations, data from the Meteonorm database for three locations (i.e. northern, central and southern Poland) are used. Details of the locations are given in Table 3, and their geographical positions are marked in Figure 6.

The highest total solar radiation on the horizontal surface during the three summer months is 455.3 kWh/m^2 and occurred at Location III, in the north of Poland. Figs. 7–9 show the distribution of ambient temperature and the total solar radiation for three PTES storage charging system locations.

RESULTS AND DISCUSSION

The total power of the PV and ST installations is estimated for three different locations in Poland by numerical calculations in the TRNSYS software. The power capacity of the installation is calculated so that the PTES heat storage tank can be charged to an average temperature of 80°C within three months. The time series of the tank temperatures are presented in Figure 10 and Figs. 13–14. In addition, Figs. 11–12 show the
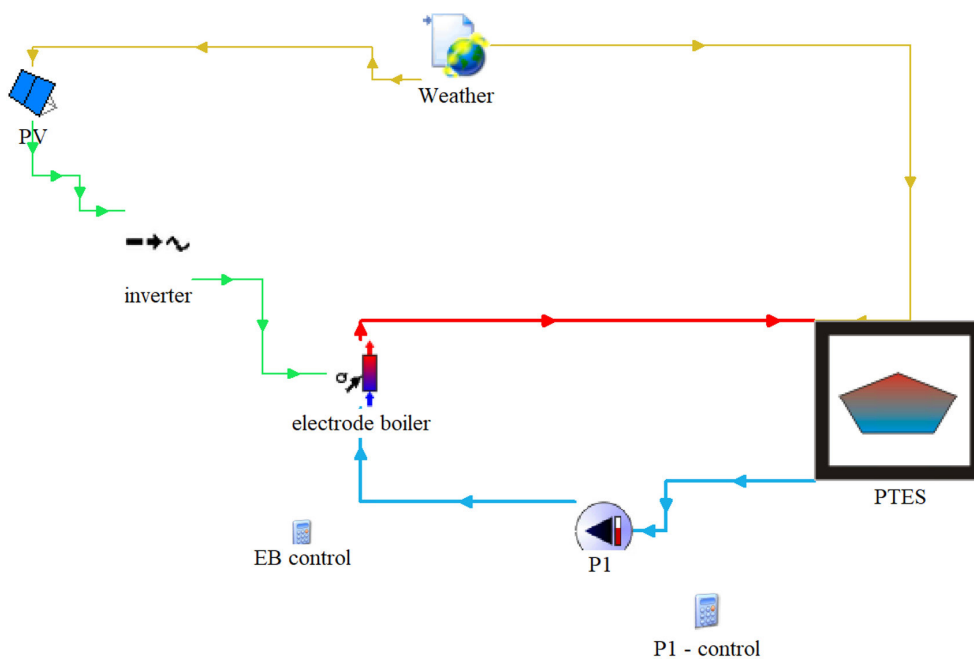

Figure 4. Schematic diagram of the PTES heat storage heating system in the TRNSYS software using photovoltaic panels (Configuration No. I)
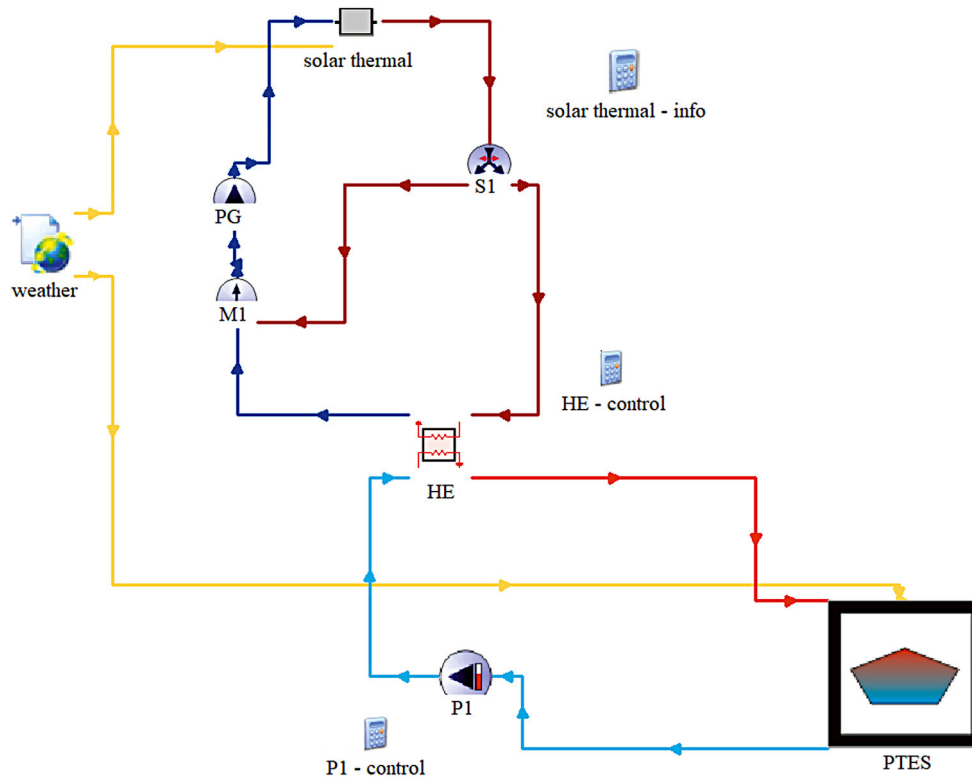
Figure 5. Schematic diagram of the PTES heat storage heating system model
using solar collectors (Configuration No. II) in the TRNSYS software.

temperature changes in the PTES over one week for Location I. Fig. 11 shows the first week and Fig. 12 the last week of charging the heat store

The first two curves (Configuration No. I – max temperature and Configuration No. II – max temperature on Figs. 10–12) refer to the maximum temperature in the PTES that occurs in the highest layer of the storage tank. At this region, the storage is charged after pre-heating the water in EB (configuration I) or HE (configuration II). In the case of Configuration No. I, the temperature increase is much more stabilised than in the case of Configuration No. II. This is because the EB continuously heats the PTES water up to 90°C. If the electricity generated by the PV is not enough to cover the EB's minimum demand, the boiler does not switch on. Otherwise, the waterflow from the PTES is selected so that the boiler can reach the fixed temperature with the available electricity. In

the case of Configuration No. II, it is much more challenging to achieve a specific temperature beyond the HE due to the varying thermal conditions on the water-glycol mixture side.

Figures 15–16 show the mass flow rate of water from the PTES to the EB (Configuration No. I) and the HE (Configuration No. II) during a single day (Fig. 15 – June 2, PTES unloaded; Fig. 16 – August 26, PTES loaded). There are significant differences between the mass flow rates in the two configurations. Water flows into the electrode boiler much lower than into the heat exchanger. However, it continues continuously throughout the day. In contrast, heat transfer in HE occurs only during the sunniest period. PTES heating is, therefore, more stabilised in Configuration No. I. In the case of a system with TS, there are much more significant fluctuations in the temperature of the upper PTES layer. This effect of both systems

Table 3. Summary of the selected location and total solar radiation per horizontal surface during the three summer months

Location	Latitude [°N]	Longitude [°E]	Total solar radiation [kWh/m²]	Average ambient temperature [°C]
Location I	52.27	20.98	440.5	17.3
Location II	50.08	19.80	449.9	16.9
Location III	54.52	18.60	455.3	15.5

Figure 6. Map showing locations of places selected for simulation

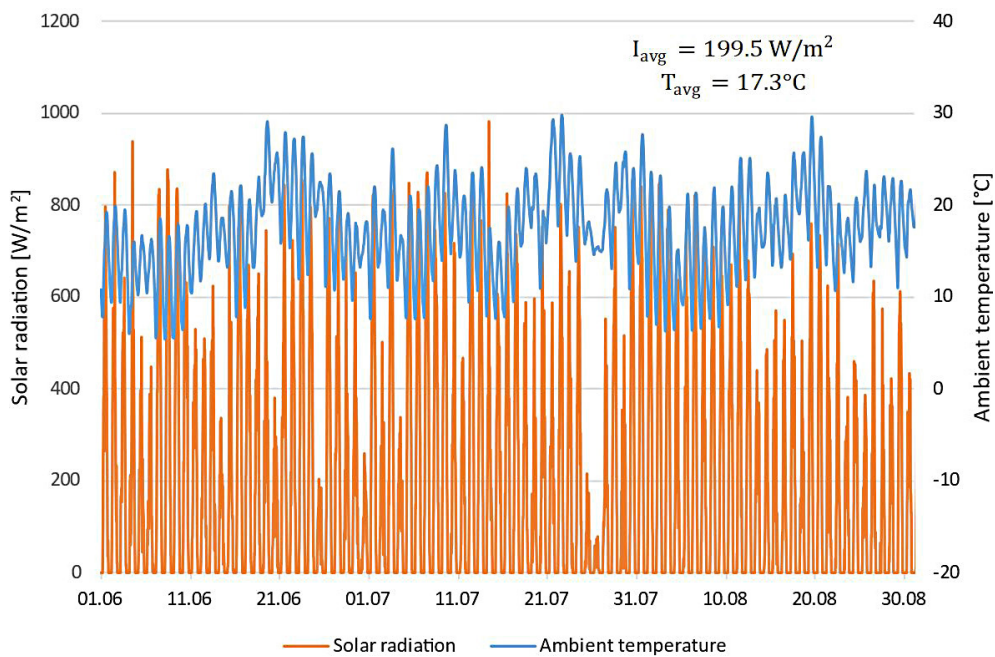$$I_{avg} = 199.5 \text{ W/m}^2$$
$$T_{avg} = 17.3°C$$

Figure 7. Distribution of ambient temperature and total solar radiation for Location I

causes the water in the upper PTES layer to heat up faster with EB and PV. This is of particular importance, considering that the water for heating when discharging the tank is drawn from the upper part of the tank.

Table 4 presents the area, rated power and estimated costs of Configuration No. I and Configuration No. II. The following indices are used to determine the investment costs: 761 EUR/kW (PV system – Configuration No. I) and 252 EUR/kW (ST system – Configuration No. II) [35]. The indices include the cost of photovoltaic panels/solar collectors and ancillary equipment.

At each location, approximately twice the installed power is needed in Configuration No. 2 compared to Configuration No. 1 to charge a 24 000 m³ PTES tank. However, the two values cannot be directly compared as they refer to different types of power. In the case of PV, the rated power is electrical power, while in the case of ST, it is thermal power.
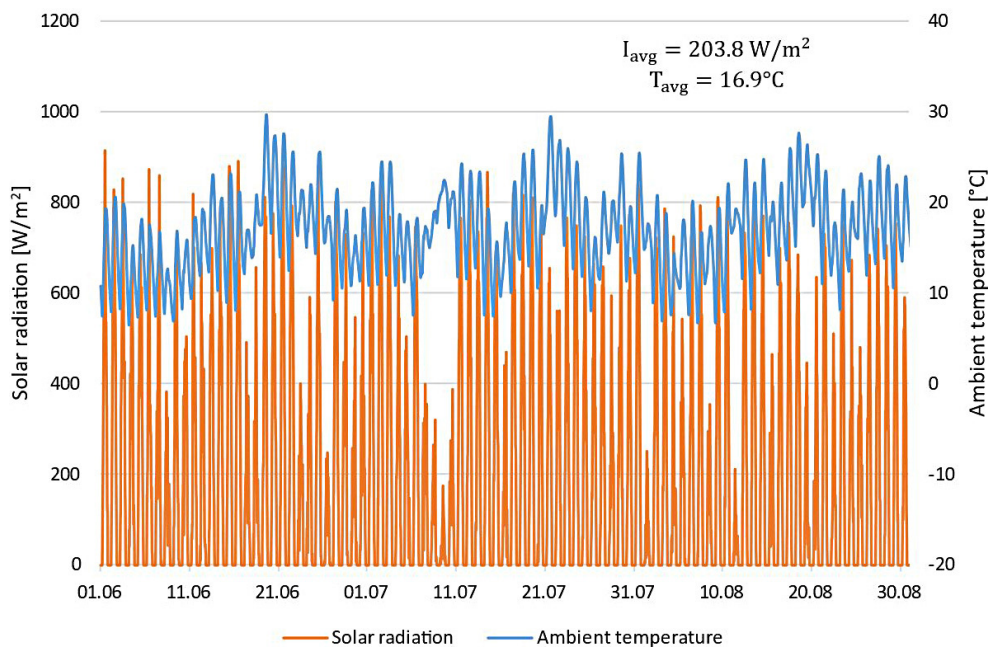
Figure 8. Distribution of ambient temperature and total solar radiation for Location II
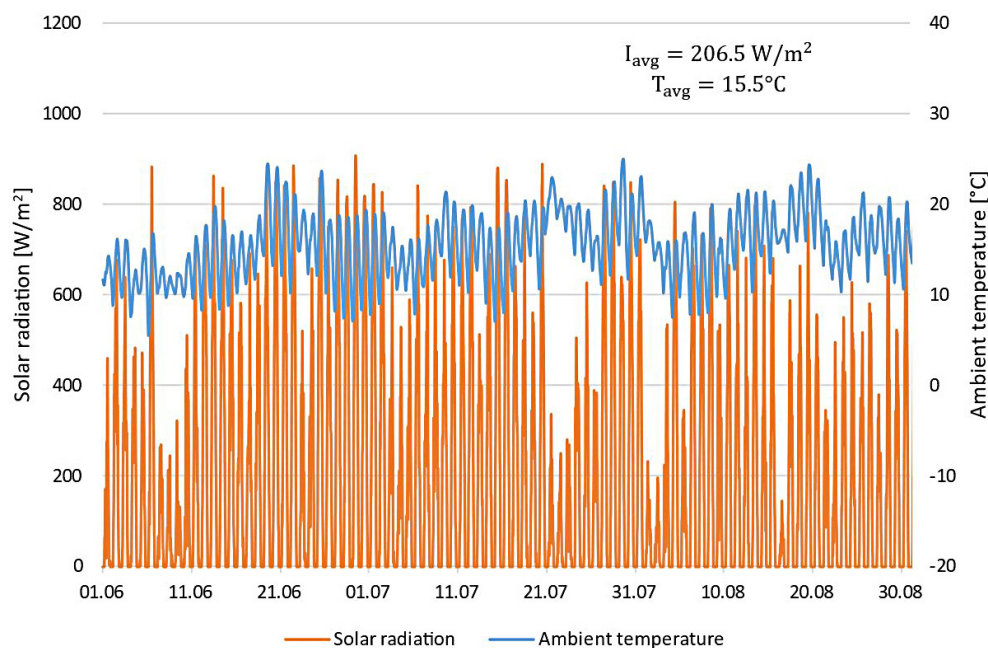

Figure 9. Distribution of ambient temperature and total solar radiation for Location III

The differences in the size of the two configurations are also because PV and ST systems behave differently depending on the weather conditions. Both transform energy when the solar radiation is high enough. However, solar thermal collectors heat the working medium even on cloudy but warm days. On the other hand, photovoltaic panels will produce energy regardless of the ambient temperature if their surface is sufficiently exposed to sunlight.

Comparing the investment costs (CAPEX), it can be seen that they are lower for the solar collector farm in all three locations. This installation also requires less available space. On the other hand, the area allocated to PV is approx. 1.5 times larger than for ST. This fact should be taken into account when considering the efficiency of the equipment. The solar collectors have a much higher efficiency in converting solar energy into heat than solar energy into electricity by PV (PV – 21.3%, ST – 77%).
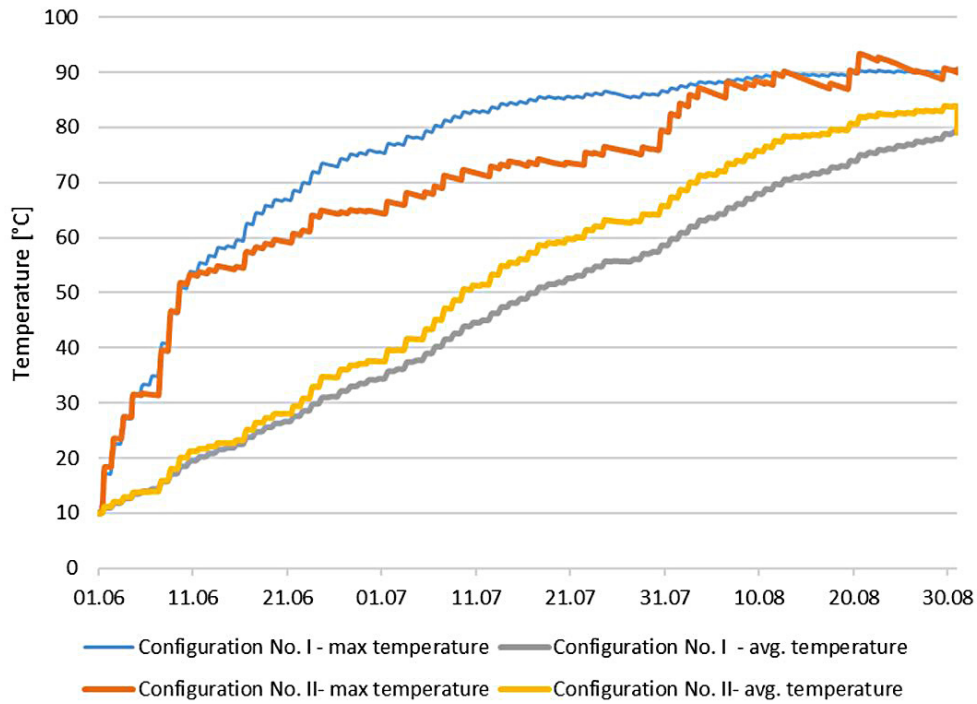
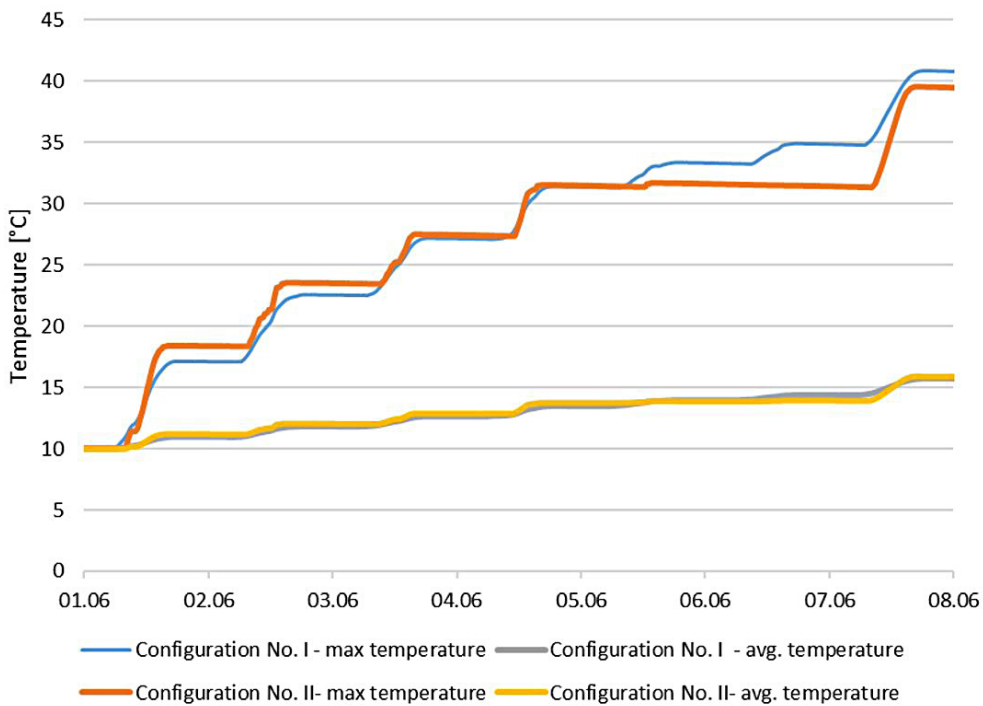**Figure 10.** Temperature distribution in the PTES at the Location I from June to August

Figure 11. Temperature distribution in the PTES at the Location I during the first week of the storage charge

Comparing the results for the three locations in Poland, it can be seen that there is a difference in the size of PV and ST systems in different locations. The largest PV and ST installation is required to be built in central Poland (location I). The minor PV system can be installed in northern Poland (location III) due to the total insolation, which is highest there. For ST, the lowest installation can be located in the southern part of the country.

The results obtained in this study confirm the findings of many previous works. Pakere et el. [36] through a multi-criteria analysis of various solar systems (PV + heat pump, solar thermal collectors, PVT + heat pump) found that in most scenarios,
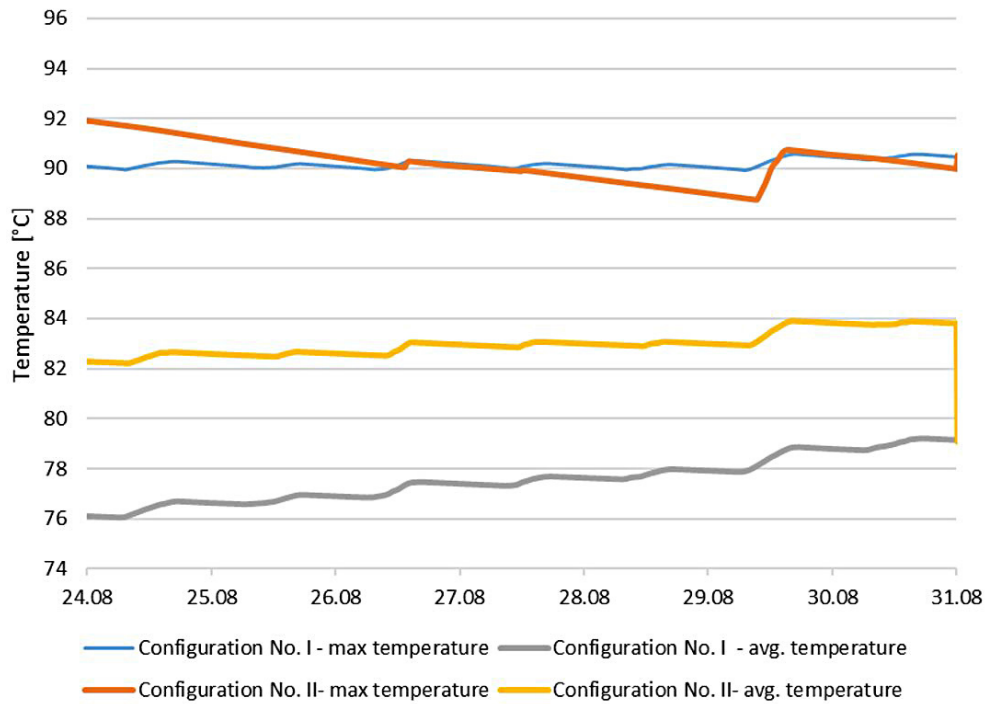
Figure 12. Temperature distribution in the PTES at the Location I during the last week of the storage charge
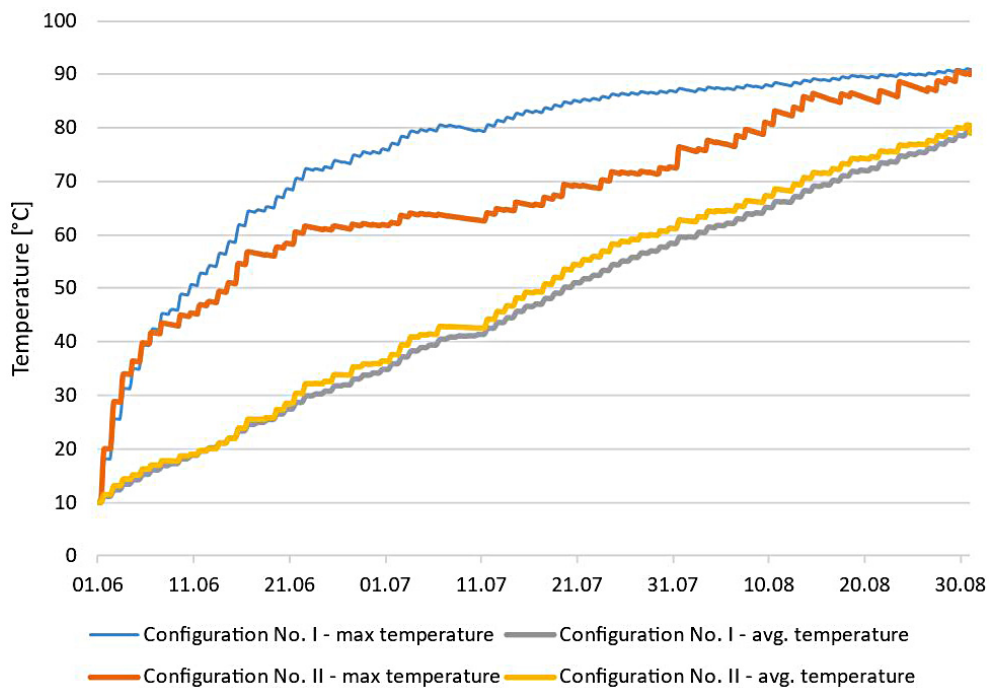

Figure 13. Temperature distribution in the PTES at the Location II from June to August

the best results were obtained for systems with ST. However, they noted the much greater flexibility of PV + P2H for multi-scale district heating systems. Similar results were also obtained by Meyers et al. [37] finding that at the prices of the time, ST are much cheaper in most regions. To now, however, no comparison has been made between the

installation of PV panels with the electrode boiler and the solar thermal farm used to charge the PTES heat storage, which is the emphasis of this paper.

In future, it is planned to implement the installation in Configuration No. 2, at which point it will be possible to verify the results obtained in practice.
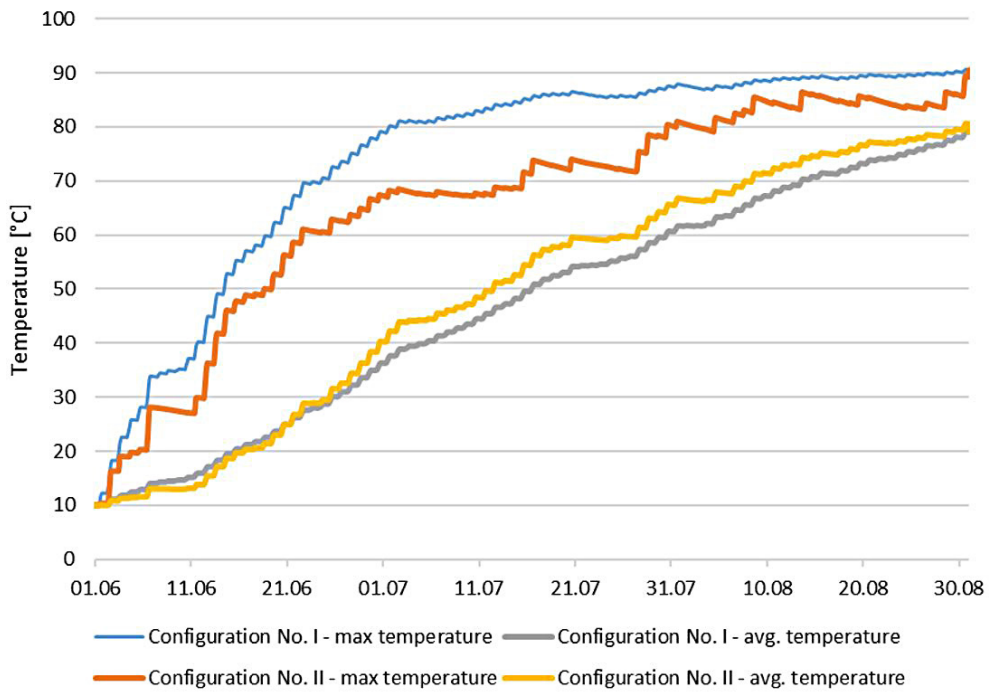
Figure 14. Temperature distribution in the PTES at the Location III from June to August
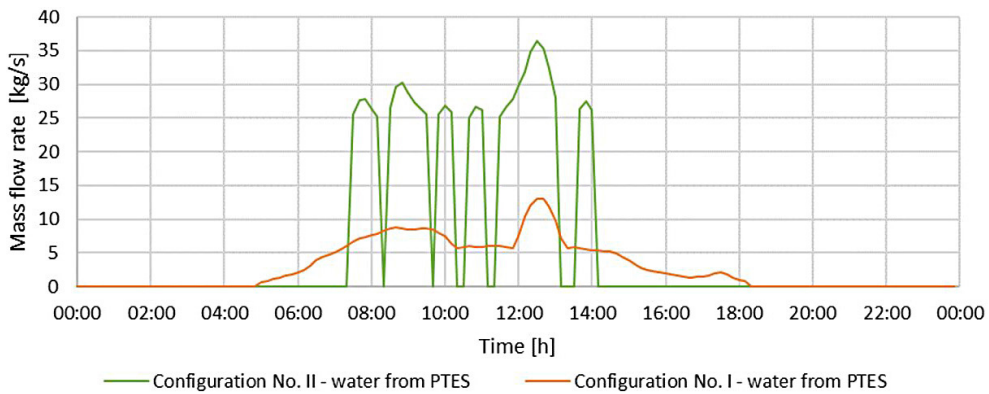

Figure 15. Mass flow rate of water from PTES to electrode boiler (Configuration No. I) and heat exchanger (Configuration No. II) on June 2
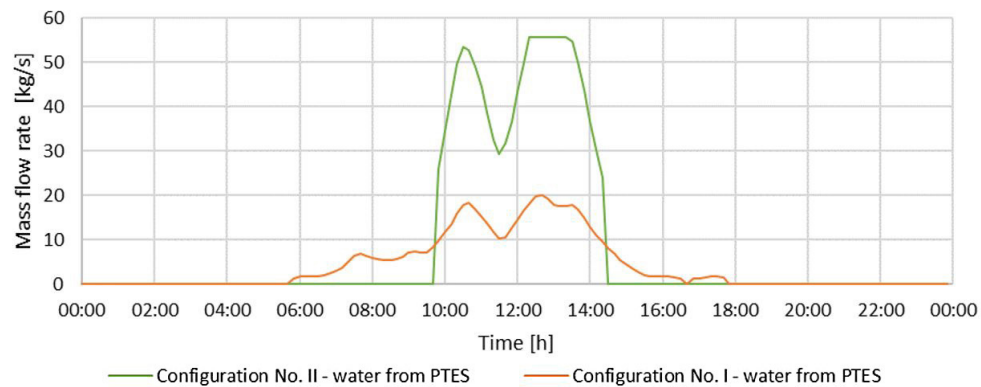

Figure 16. Mass flow rate of water from PTES to electrode boiler (Configuration No. I) and heat exchanger (Configuration No. II) on August 26

Table 4. Area, power rating and investment costs of PTES storage charging systems

Location	Parameter	Configuration No. I (PV)	Configuration No. II (ST)
Location I	Area [m²]	24861.1	16335,4
	Rated power [MW]	5.29	12.58
	Estimated investment costs [EUR]	4 026 902	3 171 900
Location II	Area [m²]	24520.5	15214.4
	Rated power [MW]	5.22	11.79
	Estimated investment costs [EUR]	3 971 739	2 973 657
Location III	Area [m²]	23567.0	15739.8
	Rated power [MW]	5.02	12.12
	Estimated investment costs [EUR]	3 817 282	3 056 259

CONCLUSIONS

The PTES energy storage in district heating can solve the mismatch between renewable energy generation and demand. PTES can be charged with solar energy using photovoltaic panels and solar collectors. However, this is a long process that takes several months, even under the most solar insolation conditions of the year. The criteria for choosing a system to charge the heat storage can be investment costs, the size of the farm and the flexibility of the installation. Based on the simulation calculations carried out, it can be concluded that, from an investment perspective, a system based on solar collectors is more cost-effective. In addition, the installation takes up less space compared to a photovoltaic panel farm.

If we consider the flexibility of the district heating system, the PV system seems to have more advantages than solar thermal. In addition to using PV to heat water (Power-to-Heat technology), excess energy can be sold or used in other ways, such as to power a heat pump. Electricity from PV is of the highest quality (exergy) and has a much more comprehensive range of applications than the heat generated by solar thermal systems. It is also essential to consider the declining price of PV, which will continue to fall in the coming years.

Acknowledgment

REFERENCES

1. Heating – Analysis – IEA [Internet]. IEA. 2021 [cited 2 April 2022]. Available from: https://www.iea.org/reports/heating

2. Owusu P.A., Asumadu-Sarkodie S. A review of renewable energy sources, sustainability issues and climate change mitigation. Cogent Engineering. 2016; 3: 1167990.

3. Exergy Flow Charts – GCEP [Internet]. Gcep.stanford.edu. [cited 4 April 2022]. Available from: http://gcep.stanford.edu/research/exergycharts.html

4. Ahamd M. State of the Art Compendium of Macro and Micro Energies. Advances in Science and Technology Research Journal. 2019; 13: 88–109.

5. França R.P., Monteiro A.C.B., Arthur R., Iano Y. Overview of sources of microgrids for residential and rural electrification: a panorama in the modern age. Residential Microgrids and Rural Electrifications. 2022; 69–85.

6. Bloess A., Schill W.-P., Zerrahn A. Power-to-heat for renewable energy integration: A review of technologies, modeling approaches, and flexibility potentials. Applied Energy. 2018; 212: 1611–1626.

7. Song Z., Ji J., Li Z. Comparison analyses of three photovoltaic solar-assisted heat pumps based on different concentrators. Energy and Buildings. 2021; 251: 111348.

8. Pakere I., Lauka D., Blumberga D. Solar power and heat production via photovoltaic thermal panels for district heating and industrial plant. Energy. 2018; 154: 424–432.

9. Allouhi A. Techno-economic and environmental accounting analyses of an innovative power-to-heat concept based on solar PV systems and a geothermal heat pump. Renewable Energy. 2022; 191: 649–661.

10. Wang D., Orehounig K., Carmeliet J. A Study of District Heating Systems with Solar Thermal Based Prosumers. Energy Procedia. 2018; 149: 132–140.

11. Tian Z., Zhang S., Deng J., Fan J., Huang J., Kong W., Perers B., Furbo S. Large-scale solar district heating plants in Danish smart thermal grid: Developments and recent trends. Energy Conversion and Management. 2019; 189: 67–80.

12. Lumbreras M., Garay R. Energy & economic assessment of façade-integrated solar thermal systems combined with ultra-low temperature district-

heating. Renewable Energy 2020; 159: 1000–1014.

13. Rehman H., Hirvonen J., Kosonen R., Sirén K. Computational comparison of a novel decentralized photovoltaic district heating system against three optimized solar district systems. Energy Conversion and Management. 2019; 191: 39–54.

14. Schmidt T., Mangold D., Müller-Steinhagen H. Central solar heating plants with seasonal storage in Germany. Solar Energy. 2004; 76: 165–174.

15. Qu W., Zhang J., Jiang R., Liu X., Zhang H., Gao Y. et al. An energy storage approach for storing surplus power into hydrogen in a cogeneration system. Energy Conversion and Management 2022; 268:116032.

16. Nielsen J.E., Sørensen P.A. Renewable district heating and cooling technologies with and without seasonal storage. Renewable Heating and Cooling. 2016; 197–220.

17. Dahash A., Ochs F., Janetti M.B., Streicher W. Advances in seasonal thermal energy storage for solar district heating applications: A critical review on large-scale hot-water tank and pit thermal energy storage systems. Applied Energy. 2019; 239: 296–315.

18. TRNSYS: Transient System Simulation Tool [Internet]. [cited 18 August 2022]. Available from: https://www.trnsys.com

19. Renaldi R., Friedrich D. Techno-economic analysis of a solar district heating system with seasonal thermal storage in the UK. Applied Energy. 2019; 236: 388–400.

20. Rosato A., Ciervo A., Ciampi G., Scorpio M., Sibilio S. Impact of seasonal thermal energy storage design on the dynamic performance of a solar heating system serving a small-scale Italian district composed of residential and school buildings. Journal of Energy Storage. 2019; 25: 100889.

21. Xu L., Guo F., Hoes P.-J., Yang X., Hensen J.L.M. Investigating energy performance of large-scale seasonal storage in the district heating system of chifeng city: Measurements and model-based analysis of operation strategies. Energy and Buildings. 2021; 247: 111113.

22. Li P., Guo F., Yang X. An inversion method to estimate the thermal properties of heterogeneous soil for a large-scale borehole thermal energy storage system. Energy and Buildings 2022; 263: 112045.

23. Narula K., Filho F.D.O., Chambers J., Patel M.K. Simulation and comparative assessment of heating systems with tank thermal energy storage – A Swiss case study. Journal of Energy Storage. 2020; 32: 101810.

24. Narula K., Filho F.D.O, Villasmil W., Patel M.K. Simulation method for assessing hourly energy flows in district heating system with seasonal thermal energy storage. Renewable Energy 2020; 151: 1250–1268.

25. Bozkaya B., Li R., Zeiler W. A dynamic building and aquifer co-simulation method for thermal imbalance investigation. Applied Thermal Engineering 2018; 144: 681–694.

26. Xie Z., Xiang Y., Wang D., Kusyy O., Kong W., Furbo S., Fan J. Numerical investigations of long-term thermal performance of a large water pit heat storage. Solar Energy. 2021; 224: 808–822.

27. Pavlov G.K., Olesen B.W. Seasonal Ground Solar Thermal Energy Storage – Review of Systems and Applications. In: Proc. of the ISES Solar World Congress, Kassel, Germany 2011, 1–11.

28. Mahon H., O'Connor D., Friedrich D., Hughes B. A review of thermal energy storage technologies for seasonal loops. Energy. 2022; 239: 122207.

29. Pit Thermal Energy Storage (PTES) [Internet]. aalborgcsp.com. [cited 4 August 2022]. Available from: https://www.aalborgcsp.com/business-areas/thermal-energy-storage-tes/pit-thermal-energy-storage-ptes/

30. Karim A., Burnett A., Fawzia S. Investigation of Stratified Thermal Storage Tank Performance for Heating and Cooling Applications. Energies. 2018; 11: 1049.

31. LONGI LR5-66HBD Product Specifications [Internet]. [cited 21 August 2022]. Available from: https://cdn.enfsolar.com/z/pp/ybp60c1bc0f796ce/757605aadaa5e711.pdf

32. ENSOL Solar collectors CATALOGUE [Internet]. [cited 21 August 2022]. Available from: https://www.ensol.pl/pdf/Catalogue2021SolarThermal-Solutions.pdf

33. ENSOL DIS150 Annex to Solar Keymark Certificate Licence Number [Internet]. 2022 [cited 21 August 2022]. Available from: https://www.dincertco.de/logos/011-7S2978%20F.pdf

34. Irshad M., Yadav A., Singh R., Kumar A. Mathematical modelling and performance analysis of single pass flat plate solar collector. IOP Conference Series: Materials Science and Engineering. 2018; 404: 012051.

35. Instytut Energetyki Odnawialnej [Internet]. [cited 21 August 2022]. Available from: https://www.ieo.pl/pl/

36. Pakere I., Lauka D., Blumberga D. Solar power and heat production via photovoltaic thermal panels for district heating and industrial plant. Energy. 2018; 154: 424–432.

37. Meyers S., Schmitt B., Vajen K. Renewable process heat from solar thermal and photovoltaics: The development and application of a universal methodology to determine the more economical technology. Applied Energy. 2018; 212: 1537–1552.